

Supplemental Material

Supplemental Methods

Cells and transfection. NIH3T3 cells were cultured as described by the American Type Culture Collection and were transfected using Lipofectamine-2000 (Invitrogen, Carlsbad, CA) according to the manufacturer's protocol with 100nM miR-15a or miR-195 mimic, control RNA, miR-15a or miR-195 inhibitor, or inhibitor control (ThermoFisher, Waltham, MA).

Southern blotting. Southern blotting for *p53* and *Arf* with genomic DNA from lymphomas was performed as previously described (1).

Luciferase assays. NIH3T3 cells were transfected (in triplicate) with luciferase reporters, β -galactosidase control plasmid, and 50nM miR-15 or miR-195 mimics or control RNA (ThermoFisher). Luciferase and β -galactosidase activity was measured 24 hours after transfection as previously described (2).

miRNA overexpression. The retroviral miRNA expression vector for miR-15a/miR-16-1 and empty retrovirus control vector (MSCV-PIG) have been previously published and were obtained from Dr. Josh Mendell (UT-Southwestern, Dallas, TX) (3).

ENCODE datasets (4). GEO33213 (GSM822290, GSM822310, GSM822301, GSM822286, GSM822291) and GEO31477 (GSM935643, GSM935491, GSM1003607).

Statistics. Student's *t*-tests (one-tailed) were used when comparing two groups. One-way ANOVA was performed with Bonferroni's correction when comparing multiple groups. Figure legends indicate the statistical tests used, what groups are being compared, and when values represent mean \pm SD or mean \pm SEM. Significance was defined as $P < 0.05$.

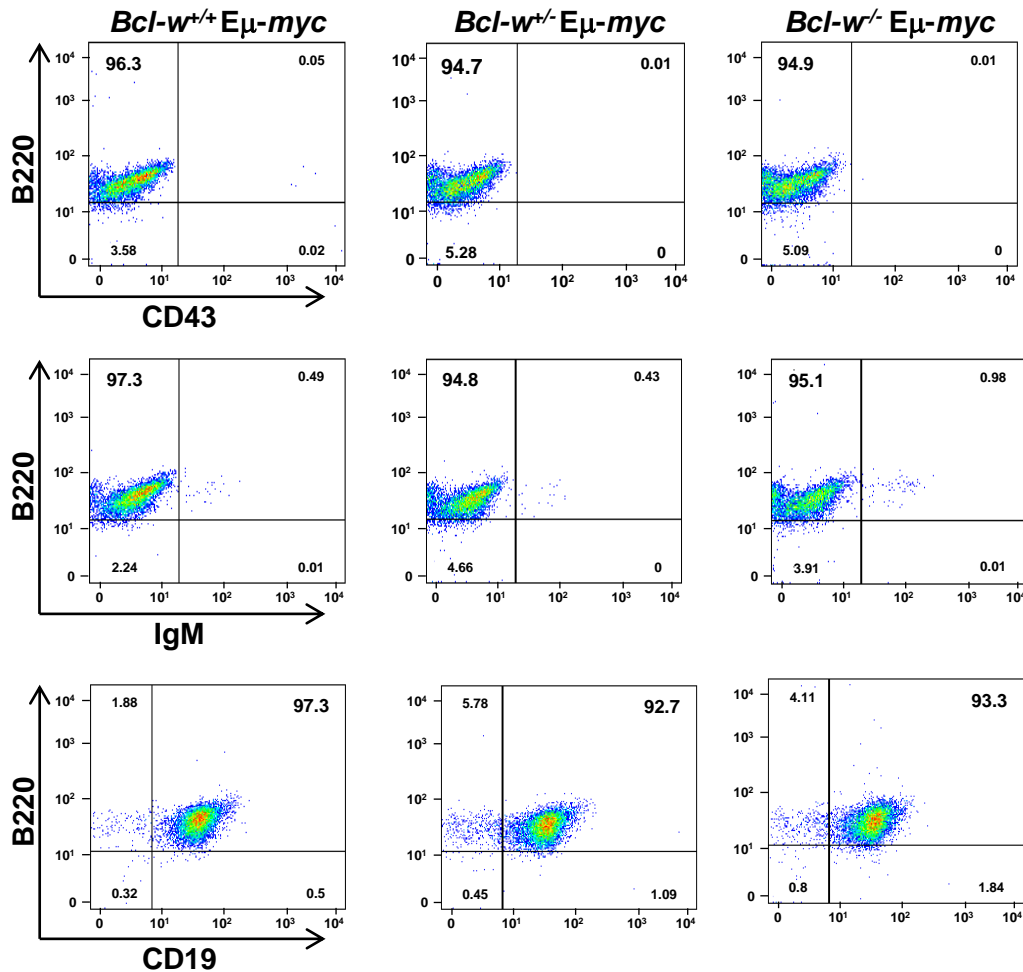
Supplemental Table 1. Expression profiling datasets analyzed for Figures 6B and 9C

	Normal samples (number)	Tumor samples (number)
GSE12195	Centroblasts (5) Centrocytes (5) Naïve B cells (5) Memory B cells (5)	DLBCL ^A (73)
GSE19246		DLBCL ^B (59)
GSE17372		DLBCL (13)
GSE26673		BL (16)
GSE64085 ^D		BL ^C (11)
GSE12453	Centroblasts (5) Centrocytes (5) Naïve B cells (5) Memory B cells (5)	BL (5) DLBCL (11)
GSE56313		DLBCL (89)
GSE12366	Germinal Center B cells (3) Naïve B cells (3) Memory B cells (3)	
Dave et. al., 2006 ^E		BL (25) DLBCL (74)

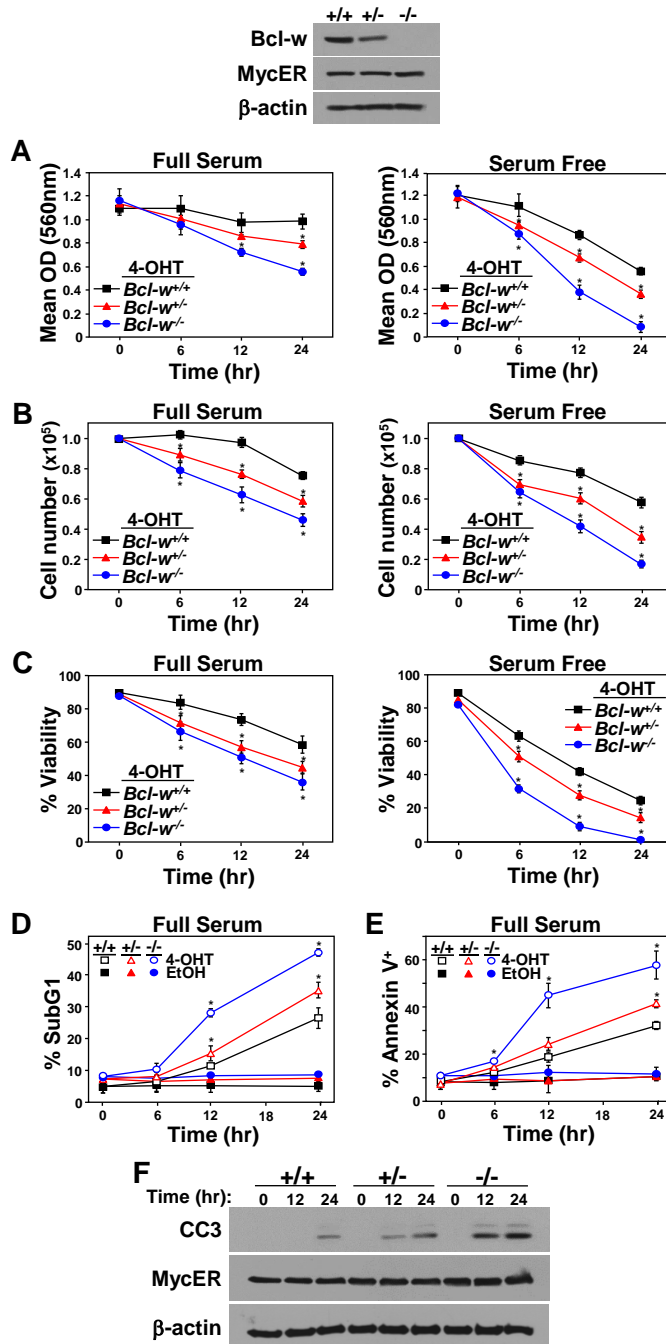
^ADLBCL, diffuse large B cell lymphoma; ^Bfresh/frozen tissue samples amplified by Eberwine oligo-dT method were analyzed; ^CBL, Burkitt lymphoma; ^Dsample GSM1564138 was excluded from the analyses because it was not used in the original publication; ^Esee supplemental ref (5)

Supplemental References

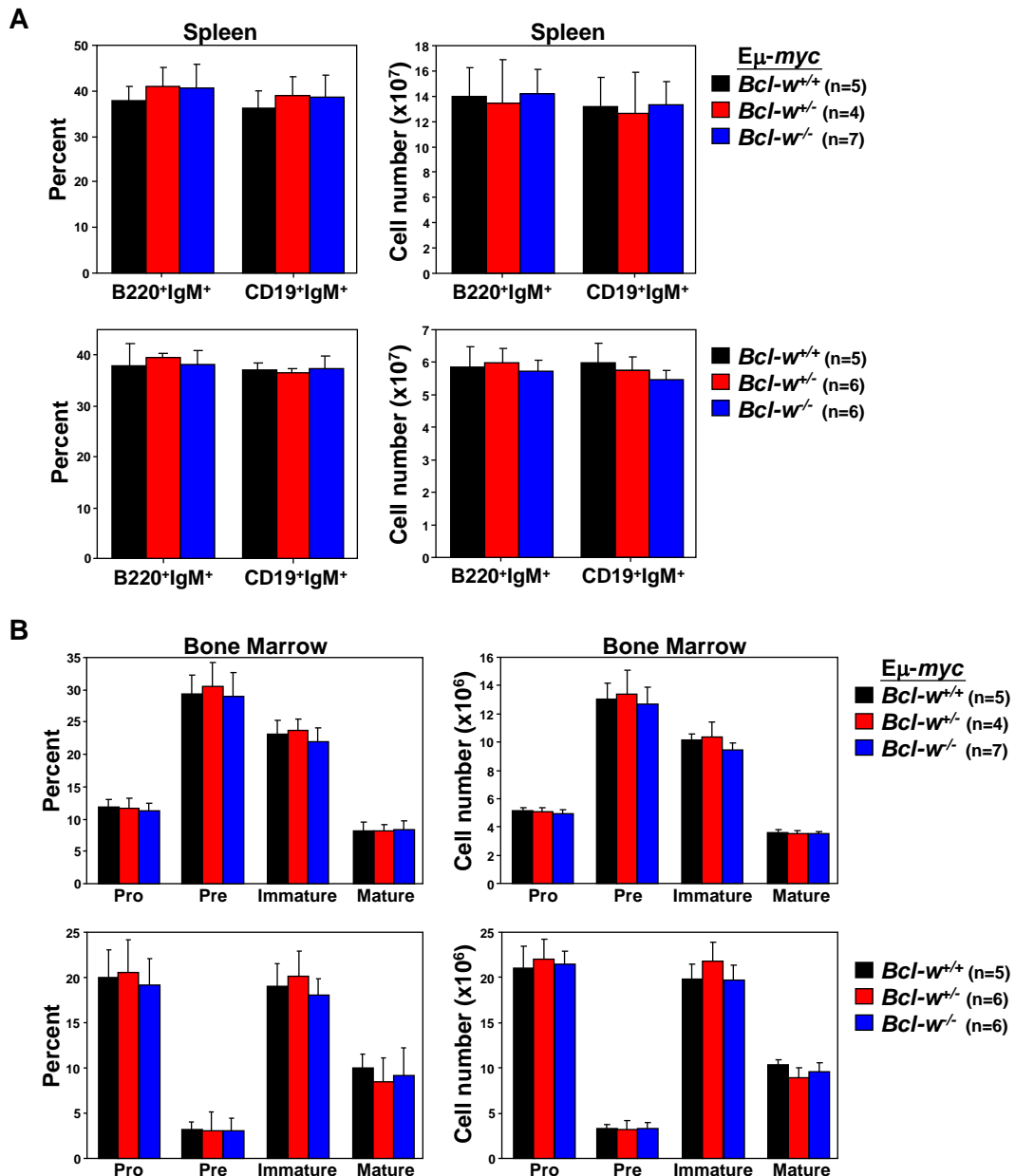
1. Eischen CM, Weber JD, Roussel MF, Sherr CJ, and Cleveland JL. Disruption of the ARF-Mdm2-p53 tumor suppressor pathway in Myc-induced lymphomagenesis. *Genes Dev.* 1999;13(20):2658-69.
2. McGirt LY, Adams CM, Baerenwald DA, Zwerner JP, Zic JA, and Eischen CM. miR-223 regulates cell growth and targets proto-oncogenes in mycosis fungoides/cutaneous T-cell lymphoma. *J Invest Dermatol.* 2014;134(4):1101-7.
3. Chang TC, Yu D, Lee YS, Wentzel EA, Arking DE, West KM, Dang CV, Thomas-Tikhonenko A, and Mendell JT. Widespread microRNA repression by Myc contributes to tumorigenesis. *Nat Genet.* 2008;40(1):43-50.
4. Consortium EP. An integrated encyclopedia of DNA elements in the human genome. *Nature.* 2012;489(7414):57-74.
5. Dave SS, Fu K, Wright GW, Lam LT, Kluin P, Boerma EJ, Greiner TC, Weisenburger DD, Rosenwald A, Ott G, et al. Molecular diagnosis of Burkitt's lymphoma. *N Engl J Med.* 2006;354(23):2431-42.



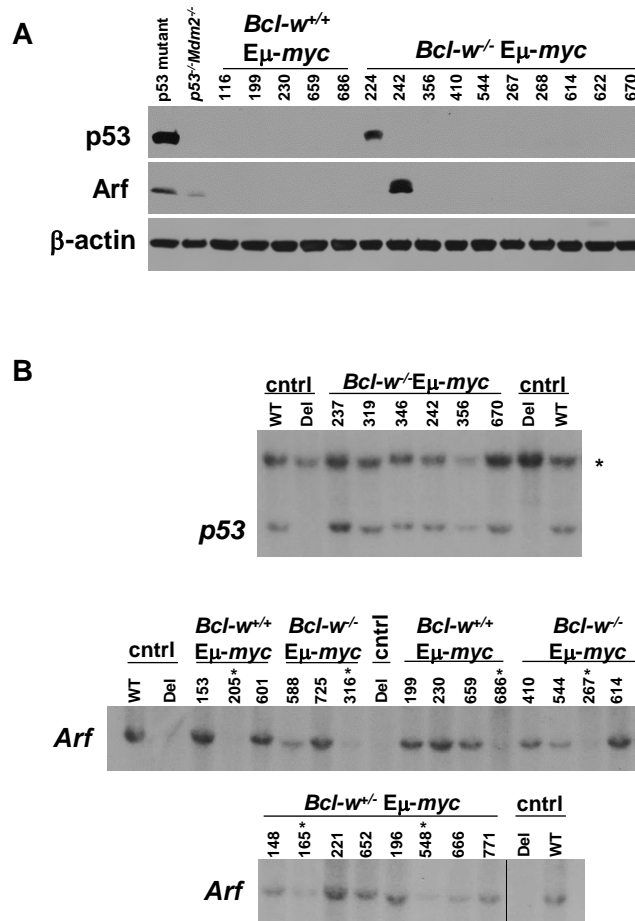
Supplemental Figure 1. Loss of *Bcl-w* does not impair B cell differentiation into pre-B cells ex vivo. Bone marrow from *Bcl-w*^{+/+}*Eμ-myc*, *Bcl-w*^{+/-}*Eμ-myc*, and *Bcl-w*^{-/-}*Eμ-myc* littermate-matched mice was placed into culture with IL-7-containing media, which selects for the outgrowth of pre-B cells. After 12 days in culture, cells were assessed for markers characteristic of pre-B cells (B220⁺ CD19⁺ CD43⁻ IgM⁻) by immunophenotyping with flow cytometry. Total lymphocytes were gated and quadrants determined using fluorochrome-linked isotype controls.



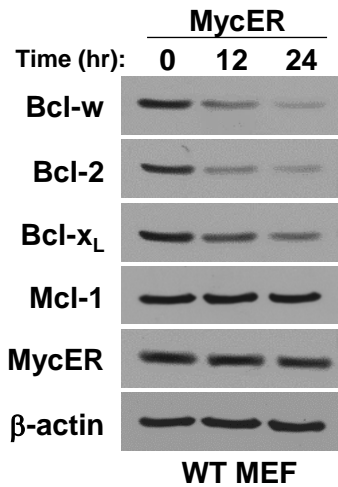
Supplemental Figure 2. Loss of *Bcl-w* increases Myc-induced apoptosis in non-hematopoietic cells. Murine embryonic fibroblasts (MEFs) were generated from *Bcl-w*^{+/+}, *Bcl-w*^{+/-}, and *Bcl-w*^{-/-} littermates and infected with a retrovirus encoding the 4-OHT inducible MycER. Following addition of vehicle (EtOH) or 4-OHT to activate MycER, MTT assays (A), total number (B), viability (C), subG1/apoptotic DNA content (PI staining, D), Annexin-V positivity (E), and appearance of Caspase 3 cleavage (CC3, F) were measured at the indicated intervals under full serum (A-C left and D-F) and serum-free (A-C right) conditions. Experiments were performed in quadruplicate (A) or triplicate (B-E) samples. Data are representative of 4 independent sets of experiments from MEFs isolated from 2 separate litters generated by different parents. Error bars are SD. **P*<0.0014 for A, **P*<0.0001 for B, and **P*<0.0001 for C; one-way ANOVA. **P*<0.008 for D and **P*<0.012 for E comparing 4-OHT treated samples; one-way ANOVA.



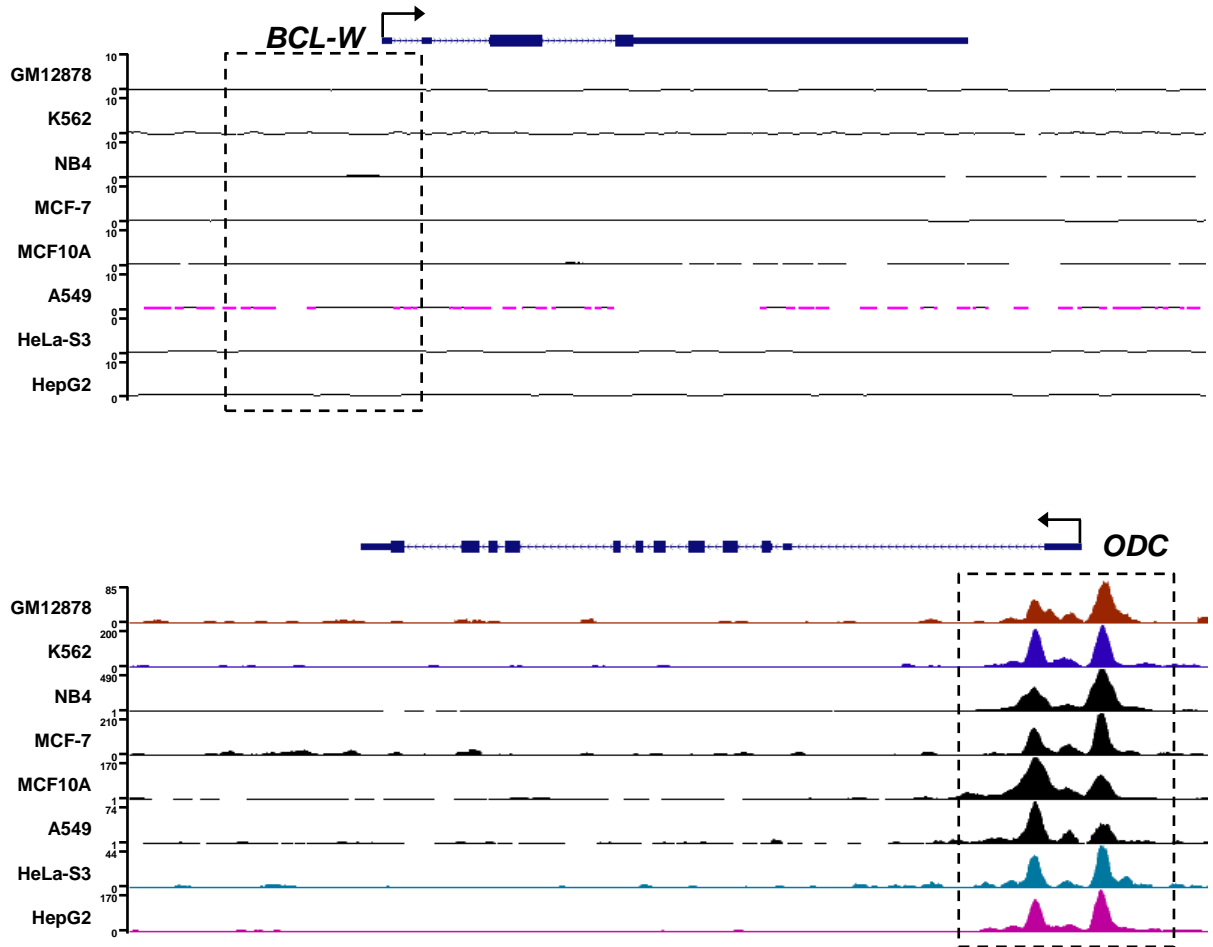
Supplemental Figure 3. *Bcl-w* deletion does not alter B cell differentiation in vivo with or without Myc overexpression. Spleens (A) and bone marrow isolated from both bones of both legs (B) from *Bcl-w*^{+/+}*E μ -myc* (n=5), *Bcl-w*^{+/-}*E μ -myc* (n=4), and *Bcl-w*^{-/-}*E μ -myc* (n=7) littermate-matched mice from four separate litters generated by different parents were isolated prior to any sign of lymphoma (top panels of A and B) or from *Bcl-w*^{+/+} (n=5), *Bcl-w*^{+/-} (n=6), and *Bcl-w*^{-/-} (n=6) littermate-matched mice from three separate litters generated by different parents (bottom panels of A and B) and subjected to immunophenotyping by flow cytometry to distinguish different B cell populations. Total lymphocytes were gated and quadrants were determined using fluorochrome-linked isotype controls. Percentages and absolute cell numbers shown. Error bars are SEM.



Supplemental Figure 4. Deletion of *Bcl-w* decreases the selective pressure to inactivate the p53 pathway during lymphomagenesis. Lymphomas from *Bcl-w*^{+/+}*Eμ-myc*, *Bcl-w*^{+/+}*Eμ-myc*, and *Bcl-w*^{-/-}*Eμ-myc* transgenic mice were subjected to Western (A) and Southern (B) blotting to determine p53 and Arf status. Controls for the Western blots include a lymphoma containing mutant p53 and *p53*^{-/-}*Mdm2*^{-/-} murine embryonic fibroblasts (MEFs). Controls (cntrl) for the Southern blots include lymphomas that contain (WT) or have deleted (Del) *p53* or *Arf*. The asterisk (*) in the *p53* Southern blot denotes the *p53* pseudogene. Lymphomas with bi-allelic *Arf* deletion are denoted by an asterisk (*). The *Arf* Southern blot in B (last panel) is from one film, and the line indicates lanes were removed. Summarized results of Western and Southern blotting are in Table 1.

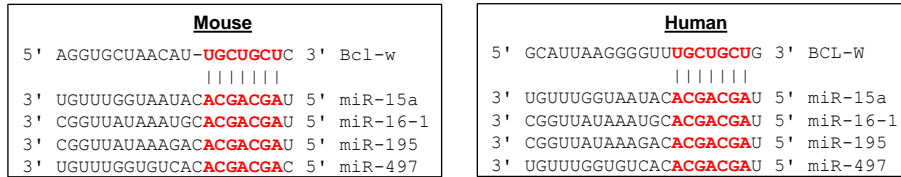


Supplemental Figure 5. Myc suppresses Bcl-w expression in non-hematopoietic cells. Wild-type murine embryonic fibroblasts (WT MEF) expressing MycER were incubated with 4-OHT to activate MycER, and cells were harvested at intervals. Western blotting was performed for the indicated proteins. Data shown is representative of 3 independent experiments.

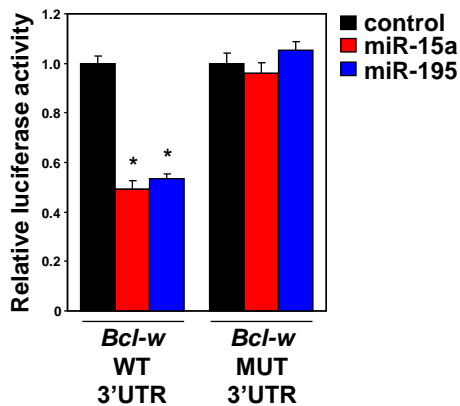


Supplemental Figure 6. MYC is not present at the *BCL-W* promoter. Evaluation of ENCODE MYC ChIP-seq data (3) demonstrates that MYC is not enriched at the *BCL-W* promoter region (dashed box) in multiple human cell lines [chronic myelogenous leukemia (K562), acute promyelocytic leukemia (NB4), lymphoblastoid (GM12878), breast cancer (MCF-7), lung adenocarcinoma (A549), cervical carcinoma (HeLa-S3), and hepatocellular carcinoma (HepG2)]. As a positive control, the same data were evaluated for MYC enrichment at the promoter of ornithine decarboxylase (*ODC*), a well-known MYC target gene. The peaks represent the fold change over that of the IgG control.

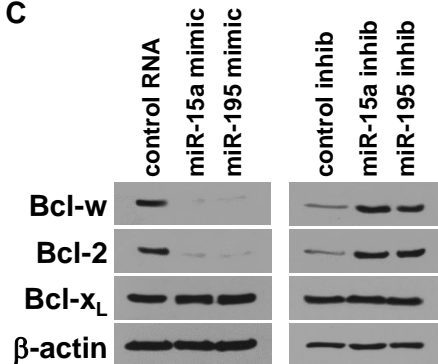
A



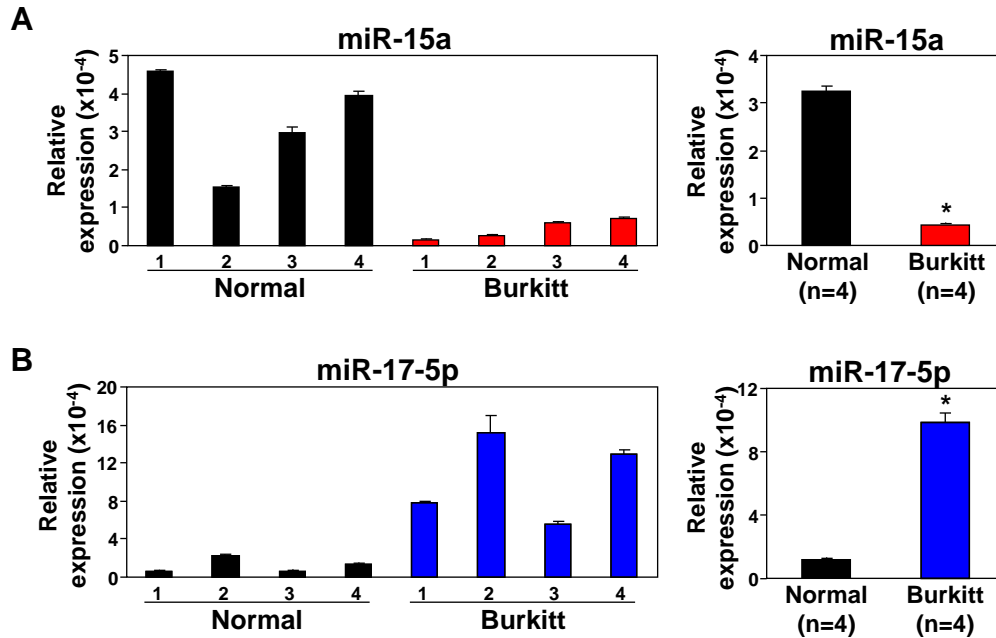
B



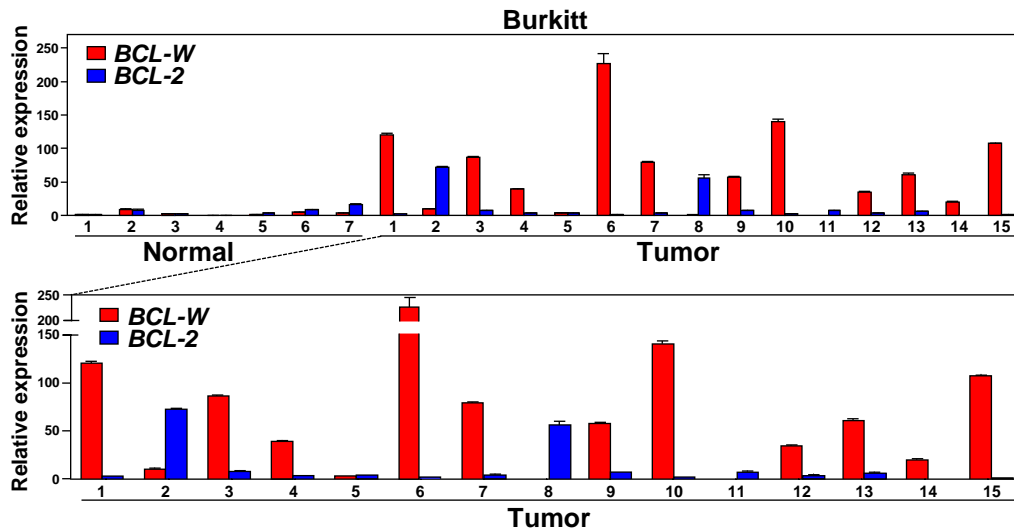
C



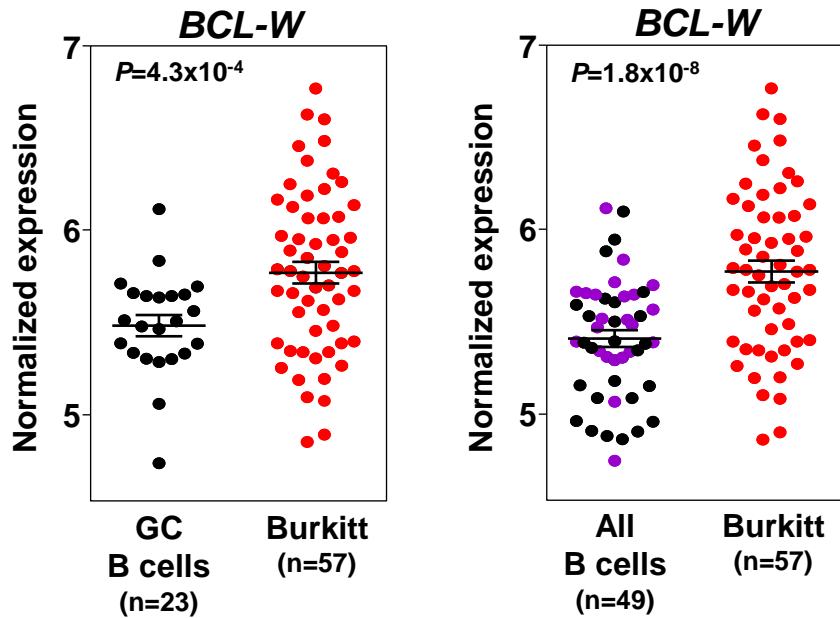
Supplemental Figure 7. *Bcl-w* is directly targeted by the miR-15 family. (A) miRNA-15 family members with the binding site of the 3'-untranslated region (3'UTR) of *Bcl-w* in mouse and human in red. (B) NIH3T3 cells were transfected with luciferase reporter plasmids containing a portion of the 3'UTR of *Bcl-w* with the miR-15 family seed sequence (WT) or the 3'UTR with a mutated miR-15 family seed sequence (MUT). miR-15a or miR-195 mimics or control RNA were also transfected in addition to a β -galactosidase reporter plasmid for transfection normalization. Luciferase activity was measured (triplicate) 24 hours after transfection. Error bars are SD. * $P < 0.0001$; one-way ANOVA. (C) Levels of the indicated proteins in NIH3T3 cells 48 hours after transfection with miR-15a mimic, miR-195 mimic, control RNA, miR-15a inhibitor (inhib), miR-195 inhibitor, or control inhibitor were determined by Western blot. Data shown is representative of 3 independent experiments.



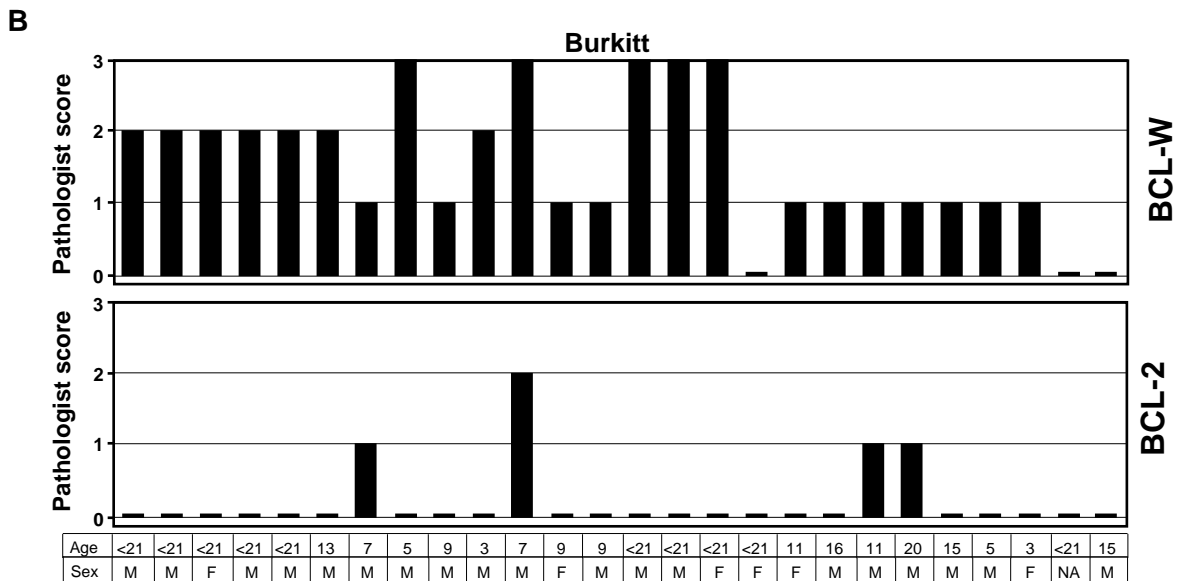
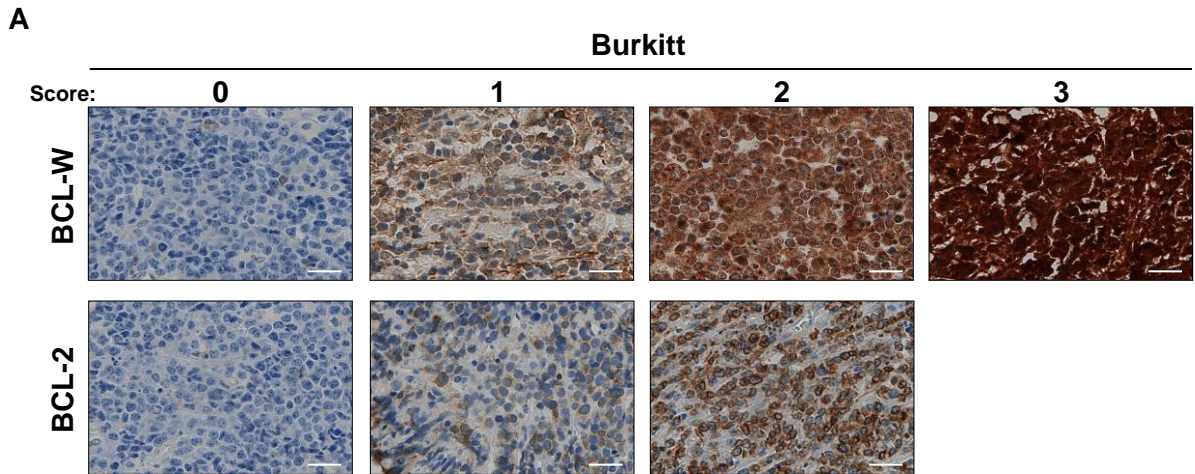
Supplemental Figure 8. miR-15a expression is decreased in Burkitt lymphoma. qRT-PCR (triplicate) was performed on patient Burkitt lymphoma samples ($n=4$) and normal lymphoid control tissue ($n=4$) for miR-15a, a representative miR-15 family member (A) and as a positive control, miR-17-5p (B), which is elevated in Myc-driven cancers. miRNA levels were normalized to the small RNA *RNU6b* and presented as $2^{-\Delta\Delta C_t}$; values for individual samples (left) and mean values (right). Error bars represent the SEM. * $P=0.019$ for A and * $P=0.008$ for B; t -tests.



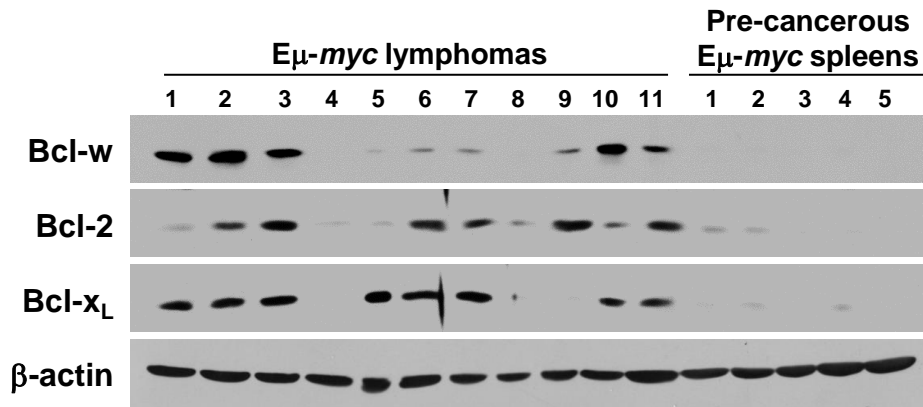
Supplemental Figure 9. *BCL-W* is overexpressed in human Burkitt lymphoma. qRT-PCR was performed in triplicate on 15 Burkitt lymphoma (BL) patient samples and 7 normal lymphoid control tissue samples. mRNA expression levels were normalized to β -*ACTIN* and presented as $2^{-\Delta\Delta C_t}$. Error bars are SEM. Results from each individual sample are presented (top panel) with the results from the lymphoma samples enlarged (bottom panel) and are the same data presented in Figure 6A in a different format.



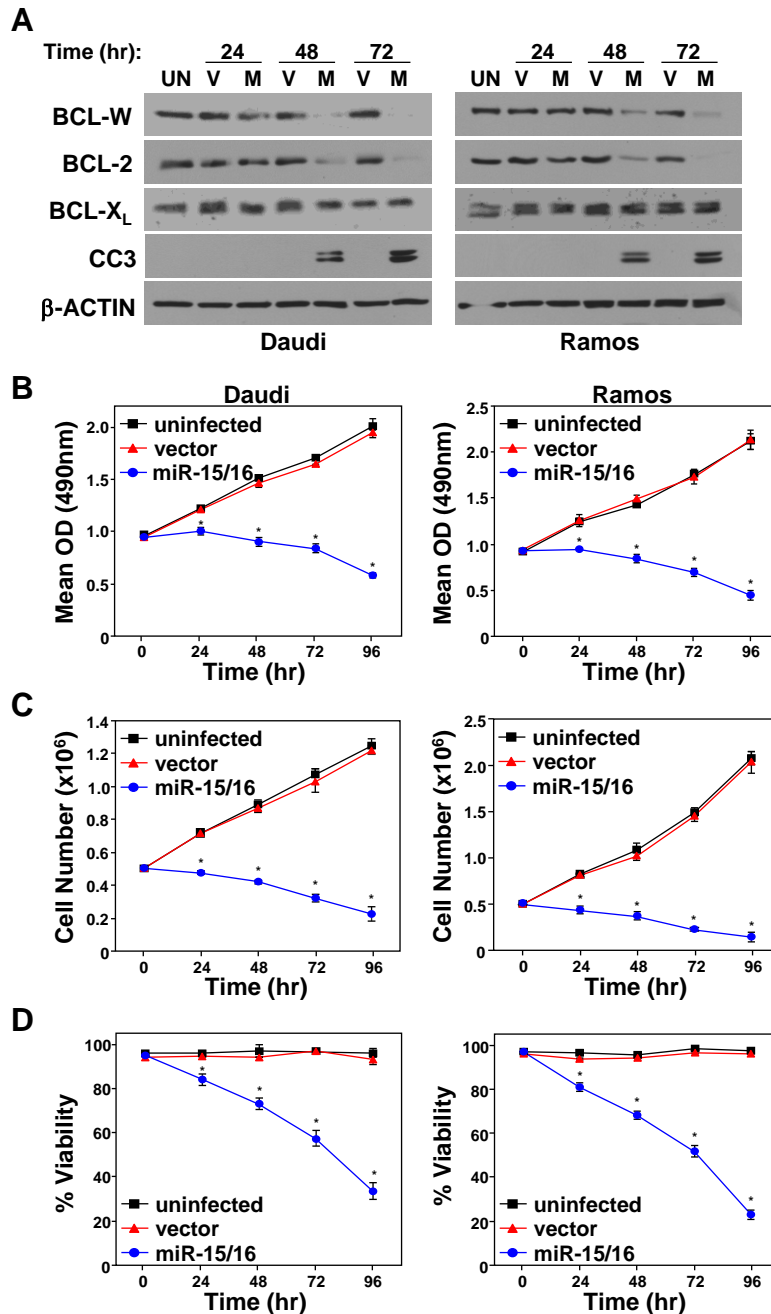
Supplemental Figure 10. Increased expression of *BCL-W* in Burkitt lymphoma compared to germinal center B cells. Microarray gene expression profiling data for *BCL-W* mRNA in Burkitt lymphoma ($n=57$) compared to only germinal center (GC) B cells ($n=23$, left) or all normal B cells evaluated ($n=49$) with GC B cells highlighted in purple (right). The data shown in the right panel is the same as the left panel in Figure 6B with the GC B cells highlighted. Lines represent the mean \pm SEM. Each circle represents one sample and the y-axis represents normalized expression of *BCL-W*. *P*-values are indicated; *t*-tests.



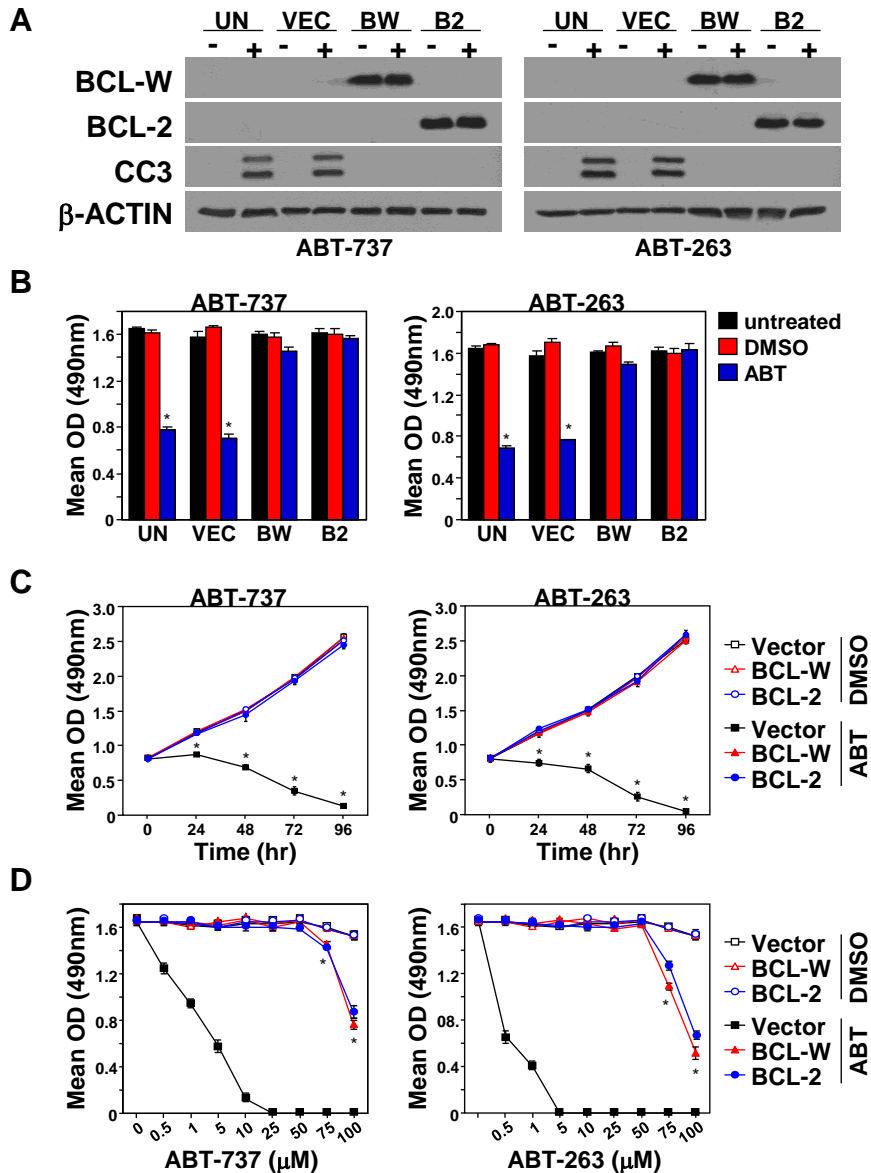
Supplemental Figure 11. Pathologist scoring of BCL-W and BCL-2 IHC in Burkitt lymphoma with individual scores and clinical characteristics. Immunohistochemistry (IHC) for BCL-W and BCL-2 was performed on human patient samples of Burkitt lymphoma ($n=26$). (A) Representative images (40x magnification, scale bar represents 200µm) of each score given by the pathologist are shown. These data illustrate the scoring used for the IHC in Figure 6C. (B) The pathologist scores for BCL-W and BCL-2 for each patient along with the patient's age and gender are indicated (M, male; F, female; NA, not available). Where duplicate/triplicate samples were available, scores were averaged and rounded to the highest integer. These data are represented in a box and whisker plot in Figure 6C.



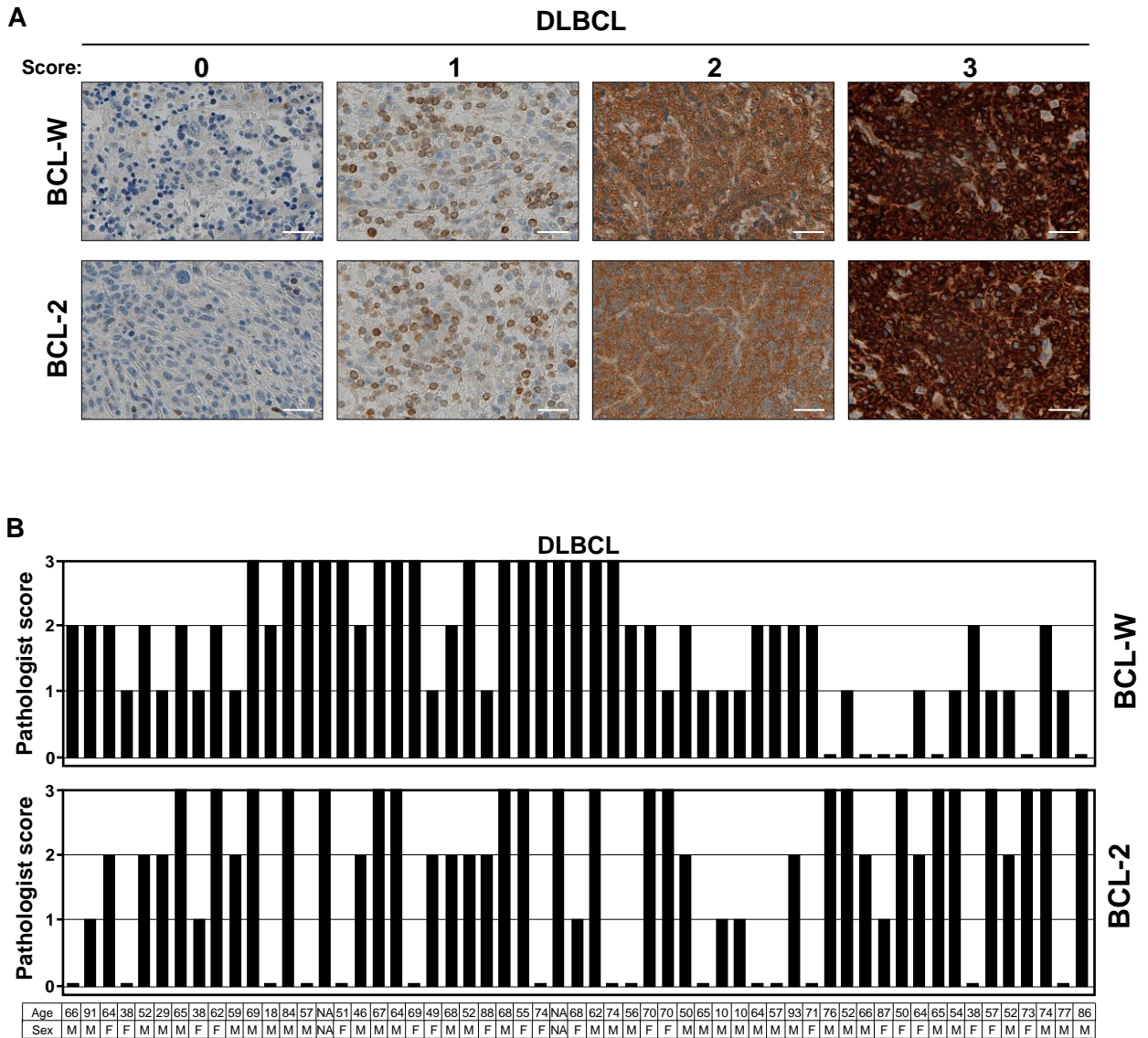
Supplemental Figure 12. Bcl-w is frequently overexpressed in *Eμ-myc* lymphomas. *Eμ-myc* lymphomas ($n=11$) and pre-cancerous *Eμ-myc* spleens ($n=5$) were Western blotted for the indicated proteins.



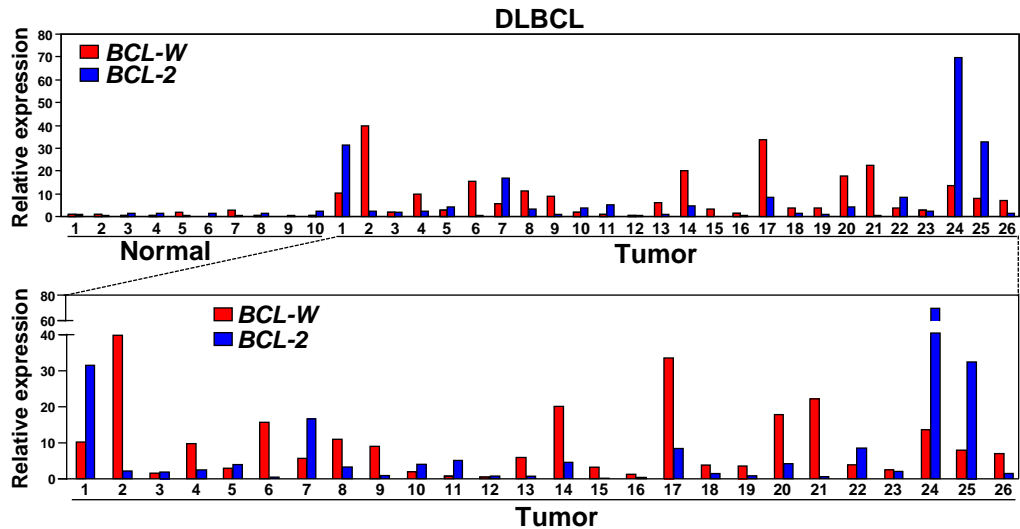
Supplemental Figure 13. Increased expression of the miR-15 family induces apoptosis in Burkitt lymphoma. Two human Burkitt lymphoma (BL) cell lines (Daudi and Ramos) remained uninfected (UN) or were infected with a retrovirus encoding empty vector (V) or the miR-15a/16-1 cluster (M). (A) Western blotting was performed for the indicated Bcl-2 family proteins and for the appearance of cleaved Caspase 3 (CC3). Equal number of cells were placed in culture and MTS assays (B), total cell number (C), and viability (D) were measured at the indicated intervals. Experiments were performed in quadruplicate (B) or triplicate (C and D) samples. Data are representative of 2 independent experiments for each of the cell lines. Error bars are SD. * $P < 0.001$ for B, * $P < 0.0033$ for C, and * $P < 0.0063$ for D comparing miR-15/16 to vector; t -tests.



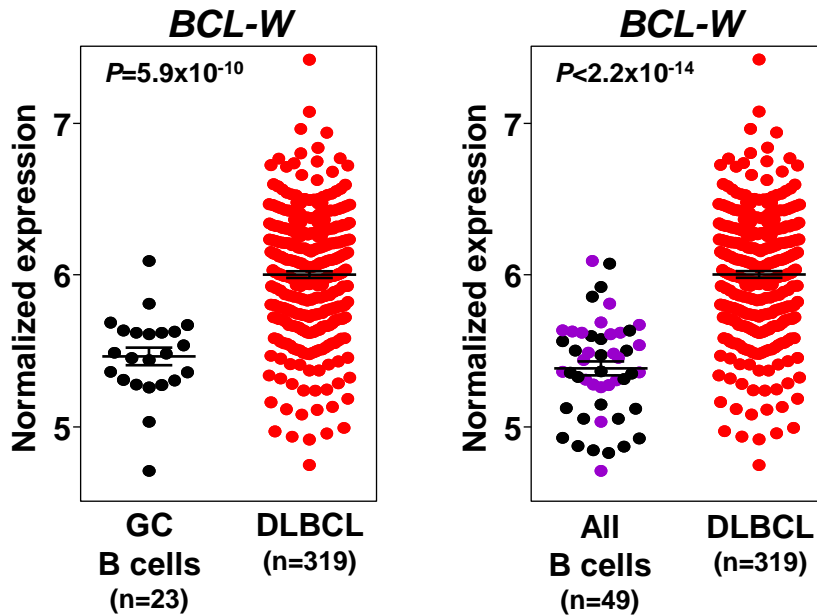
Supplemental Figure 14. Increased expression of BCL-W confers resistance to Burkitt lymphoma cells to BH3-mimetics. The human Burkitt lymphoma cell line Ramos was left uninfected (UN) or was retrovirally infected to express BCL-W (BW), BCL-2 (B2), or empty vector (VEC). Following treatment with ABT-737 (left, +), ABT-263 (right, +), or vehicle control (DMSO, -) at the IC_{50} determined in Figure 8A (A-C) or the indicated concentrations (D) for 48 hrs (A, B, and D) or the indicated intervals (C), Western blotting (A; cleaved Caspase 3, CC3) and MTS assays (B-D; quadruplicate) were performed. Data shown are representative of 2 independent experiments for both inhibitors. For data shown in B, C, and D, experiments with the inhibitors were performed at the same time but graphed separately and thus, the DMSO control data are the same. Error bars are SD. * $P < 9.52 \times 10^{-6}$ ABT-737 and * $P < 8.17 \times 10^{-6}$ ABT-263 for B (ABT vs. DMSO); * $P < 7.45 \times 10^{-5}$ ABT-737 and * $P < 2.12 \times 10^{-4}$ ABT-263 for C (vector with ABT vs. vector, BCL-W, or BCL-2 with DMSO); * $P < 0.0026$ ABT-737 and * $P < 3.6 \times 10^{-5}$ ABT-263 for D (BCL-W or BCL-2 with ABT vs. BCL-W or BCL-2 with DMSO); *t*-tests.



Supplemental Figure 15. Pathologist scoring of BCL-W and BCL-2 IHC in DLBCL with individual scores and clinical characteristics. Immunohistochemistry (IHC) for BCL-W and BCL-2 was performed on human patient samples of diffuse large B cell lymphoma (DLBCL, *n*=57). (A) Representative images (40x magnification, scale bar represents 200µm) of each score given by the pathologist are shown. These data illustrate the scoring used for the IHC for Figure 9A. (B) The pathologist scores for BCL-W and BCL-2 for each patient along with the patient’s age and gender are indicated (M, male; F, female; NA, not available). Where duplicate/triplicate samples were available, scores were averaged and rounded to the highest integer. These data are represented in a box and whisker plot in Figure 9A.



Supplemental Figure 16. *BCL-W* is overexpressed in human DLBCL. qRT-PCR was performed on 26 patient samples of diffuse large B cell lymphoma (DLBCL) and 10 samples from normal lymphoid tissue (normal samples: 1 and 3-6 are lymph node; 2 and 7-10 are spleen). mRNA expression levels were normalized to β -*ACTIN* and presented as $2^{-\Delta\Delta Ct}$. Results from each individual sample are presented (top panel) with the results from the lymphoma samples enlarged (bottom panel) and are the same data presented in Figure 9B in a different format.



Supplemental Figure 17. Increased expression of *BCL-W* in DLBCL compared to germinal center B cells. Microarray gene expression profiling data for *BCL-W* mRNA in diffuse large B cell lymphoma (DLBCL, $n=319$) compared to only germinal center (GC) B cells ($n=23$, left) or all normal B cells evaluated ($n=49$) with GC B cells highlighted in purple (right). The data shown in the right panel is the same as the left panel in Figure 9C with GC B cells highlighted. Lines represent the mean \pm SEM. Each circle represents one sample and the y-axis represents normalized expression of *BCL-W*. *P*-values are indicated; *t*-tests.